Mechanical Systems and Signal Processing 54-55 (2015) 405–416

Contents lists available at ScienceDirect

Mechanical Systems and Signal Processing

journal homepage: www.elsevier.com/locate/ymssp

Energy harvesting in a nonlinear piezomagnetoelastic beam subjected to random excitation

Aline S. De Paula [a,*], Daniel J. Inman [b], Marcelo A. Savi [c]

[a] Department of Mechanical Engineering, Universidade de Brasília, 70.910.900 Brasília, DF, Brazil
[b] Department of Aerospace Engineering, University of Michigan, Ann Arbor, MI, USA
[c] COPPE, Department of Mechanical Engineering, Universidade Federal do Rio de Janeiro, P.O. Box 68.503, 21.941.972 Rio de Janeiro, RJ, Brazil

ARTICLE INFO

Article history:
Received 16 October 2013
Received in revised form
13 August 2014
Accepted 22 August 2014
Available online 26 September 2014

Keywords:
Piezoelectric material
Energy harvesting
Random excitation
Nonlinearities

ABSTRACT

This work addresses the influence of nonlinearities in energy harvesting from a piezomagnetoelastic structure subjected to random vibrations. Nonlinear equations of motion that describe the electromechanical system are given along with theoretical simulations. The numerical analysis presents a comparison between the voltage provided from a linear, nonlinear bistable and nonlinear monostable systems due to random vibration. Experimental performance of the generator exhibits qualitative agreement with the theory, showing an enhancement of piezoelectric power generation in a bistable system when it vibrates around both stable equilibrium points. A relationship between variations in the excitation and a bistable system response is established from numerical simulations, defining a region of enhanced power generation when compared to the linear and nonlinear monostable cases.

1. Introduction

Energy harvesting is a concept where available energy is converted into electrical energy that can be used or stored. This idea is very useful for applications in powering small electronic devices. Mechanical vibration energy harvesting can combine this general concept with vibration reduction purposes, eliminating undesirable vibrations to generate useful energy. Piezoelectric elements are essential in this process establishing the mechanical–electrical coupling.

Vibration-based energy harvesting using piezoelectric material has been mainly focused on systems subjected to harmonic excitations. In this case, the best performance is achieved when the system is excited in its fundamental resonance. If the excitation frequency is changed slightly, the power output is drastically reduced. Thus, there have been research efforts focused on the concept of broadband energy harvesting to overcome this drawback [1–5] and some of them explore nonlinear bistable energy converters [6–8]. In this regard, Erturk et al. [9] showed that broadband behavior can be obtained by exploring nonlinearities of a bistable piezomagnetoelastic structure subjected to harmonic excitation. Ferrari et al. [10,11] investigated the same piezomagnetoelastic system studied by Erturk et al. [9] when subjected to random excitation. As in the case with harmonic excited system, the authors showed that the energy harvested could be enhanced by the presence of nonlinearities, depending on the excitation.

* Corresponding author.
E-mail addresses: alinedepaula@unb.br (A.S. De Paula), daninman@umich.edu (D.J. Inman), savi@ufrj.br (M.A. Savi).

http://dx.doi.org/10.1016/j.ymssp.2014.08.020
0888-3270/

The goal of the analysis presented here is to establish the appropriate excitation to lead to the increase of power output in vibration-based energy harvesting system subjected to random excitations. A piezomagnetoelastic structure under random excitation is investigated considering the influence of nonlinearities. A comparative analysis between linear, nonlinear bistable and nonlinear monostable systems is carried out by both numerical and experimental approaches. Since the bistable system can enhance the harvested energy when the system vibrates around both equilibrium points [10,11], an analysis is carried out with the goal of defining appropriate excitations that lead to an enhanced power output. This desired range is established by defining a relationship between the variance of excitation and the potential energy.

2. Piezomagnetoelastic nonlinear converter

The energy harvesting system is a magnetoelastic structure that consists of a ferromagnetic cantilevered beam with two permanent magnets, one located in the free end of the beam and the other at a vertical distance d from the beam free end, subjected to random base excitation. In order to use this device as a piezoelectric power generator, two piezoceramic layers are attached to the root of the cantilever and a bimorph generator is obtained as depicted in Fig. 1a. The correspondent experimental rig is shown in Fig. 1b.

The PZT layers are connected to an electrical load (a resistor for simplicity) and the voltage output of the generator across the load due to seismic excitation is the primary interest in energy harvesting. The electromechanical system behavior is approximated by the following equations of motion where x is the dimensionless tip displacement of the beam in transverse direction, ζ is the mechanical damping ratio, f_0 is the dimensionless magnitude of excitation and forcing function $n(t)\sim N(1,0)$ is a Gaussian white noise; β and α are respectively, the linear and the nonlinear stiffness coefficients; and an overdot represents differentiation with respect to dimensionless time. Erturk and Inman [12,13] and Erturk et al. [9,14] showed details of the formulation expressed by the following equation:

$$\ddot{x}+2\zeta\dot{x}+\beta x+\alpha x^3-\chi v=f_0 n(t) \tag{1}$$

$$\dot{v}+\lambda v+\kappa\dot{x}=0 \tag{2}$$

where v is the dimensionless voltage across the load resistance, χ is the dimensionless piezoelectric coupling term in the mechanical equation, κ is the dimensionless piezoelectric coupling term in the electrical circuit equation, and λ is the reciprocal of the dimensionless time constant ($\lambda=1/R_l C_p$, where R_l is the load resistance and C_p is the equivalent capacitance of the piezoceramic layers).

Note that β defines the equivalent beam stiffness and magnet force, while α is defined uniquely by the magnet force. The values of β and α define the representation of different dynamical systems. In terms of equilibrium points, it is possible to observe saddle points, represented by subscript SAD, and stable spiral, represented by subscript SEP. Hence, if $\beta<0$, the system is bistable with three equilibrium points: $(x_{SAD},\dot{x}_{SAD})=(0,0)$ (a saddle) and $(x_{SEP},\dot{x}_{SEP})=(\pm\sqrt{-\beta/\alpha},0)$ (two stable spirals for $0<\zeta<1$). If $\beta\geq 0$ and $\alpha>0$, the system is nonlinear monostable and the equilibrium point is $(x_{SEP},\dot{x}_{SEP})=(0,0)$ (stable spiral). On the other hand, if $\beta\geq 0$ and $\alpha=0$, the system is linear and has the same equilibrium point as the monostable case. These different dynamical systems can be observed by evaluating the potential energy function, presented in Eq. (3), in a range of the tip displacement x, as shown in Fig. 2. Note the difference between single well and double well potentials.

$$U(x)=\frac{1}{2}\beta x^2+\frac{1}{4}\alpha x^4 \tag{3}$$

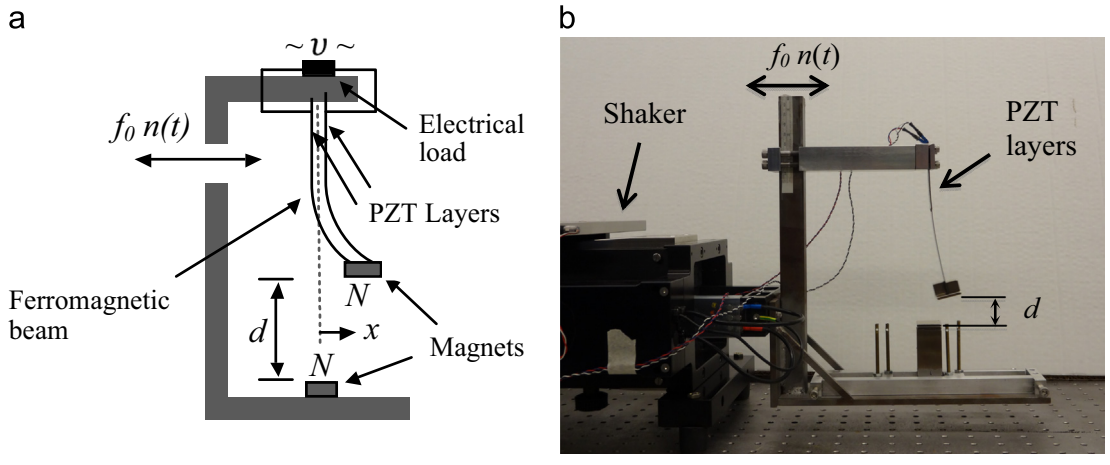

Fig. 1. Piezomagnetoelastic energy harvester set up. (a) Schematic and (b) experimental rig.

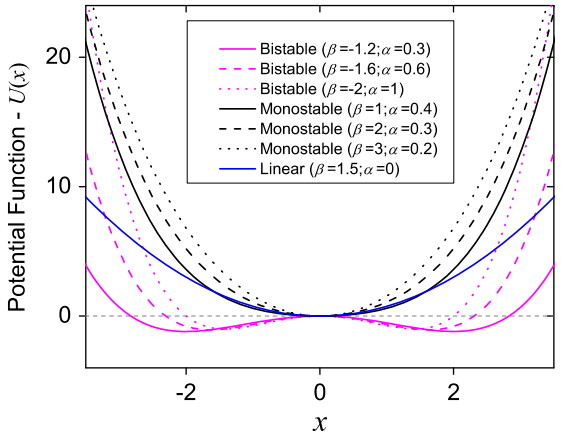

Fig. 2. Potential function for different values of β and α.

The bistable system's behavior is such that the tip of the beam can either oscillate around one equilibrium point, visiting only one well for suitable small excitations, or it can jump between the wells if the supplied mechanical energy is high enough [10,11]. The jumps between wells result in an average increase of the power supplied by the converter. Thus, it is interesting to define the range of excitations such that the tip oscillates around both stable equilibrium points (SEP). In this regard, the potential energy of the symmetric double well, U_{SEP}, is an important quantity of the system since the provided energy has to be enough to make the system jump from one well to the other. This potential is given by the following equation:

$$U_{SEP} = \frac{1}{2}\beta x_{SEP}^2 + \frac{1}{4}\alpha x_{SEP}^4 \tag{4}$$

The performance of the piezomagnetoelastic structure is evaluated by the RMS voltage and by the efficiency in power conversion:

$$\eta = \frac{p_e}{p_m} 100 \quad [\%] \tag{5}$$

where p_e and p_m are, respectively, the electrical and the mechanical power effective value. The power effective value is defined as follows:

$$p = \sqrt{\frac{1}{t}\int_o^t \left(p^{ins}\right)^2 dt} \tag{6}$$

where p^{ins} is the instantaneous power and t is the time.

The instantaneous dimensionless electrical power harvested by the piezomagnetoelastic structure is defined as the product of voltage and current:

$$p_e^{ins} = \upsilon i \tag{7}$$

where $i = \lambda\upsilon$ is the dimensionless current.

The instantaneous dimensionless mechanical power is then:

$$p_m^{ins} = \dot{x} f_0 \tag{8}$$

Numerical simulations and experimental analysis of this energy harvesting system is treated in the following analysis, showing the main characteristics of the system dynamics.

2.1. Numerical simulations

Initially, numerical analysis of the energy harvesting system is carried out by considering $\zeta = 0.01$, $\chi = 0.05$, $\kappa = 0.5$ and $\lambda = 0.05$, the same parameters considered in [9]. For initial conditions, the system is considered to be at rest at a stable equilibrium point. We investigate the RMS voltage obtained from the magnetopiezoelastic structure and the efficiency in power conversion in linear, nonlinear bistable and nonlinear monostable cases for different values of excitation magnitude, f_0. For each set of parameters the simulation is carried out 50 times and the average values are presented. Fig. 3 shows the power spectral density (PSD) of $n(t)$ showing that it is spread over the frequency values.

Fig. 4 presents the RMS voltage with respect to the forcing magnitude, f_0, obtained from linear, nonlinear bistable and nonlinear monostable systems, while Fig. 5 presents the same quantities with respect to the variance, σ^2, of the excitation $f_0\, n(t)$. Comparing Figs. 4 and 5, we note that a higher variance is related to a higher forcing magnitude, f_0. This happens

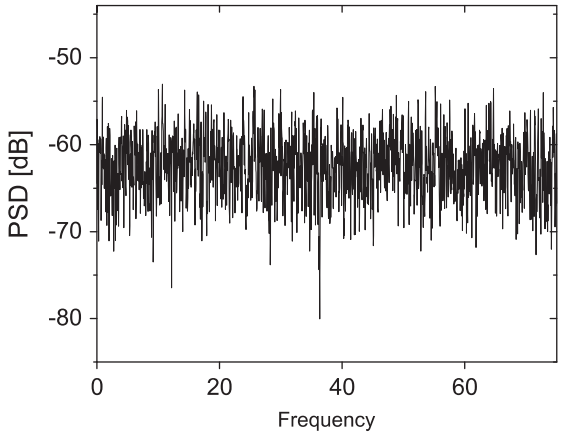

Fig. 3. PSD of the forcing function $n(t)$.

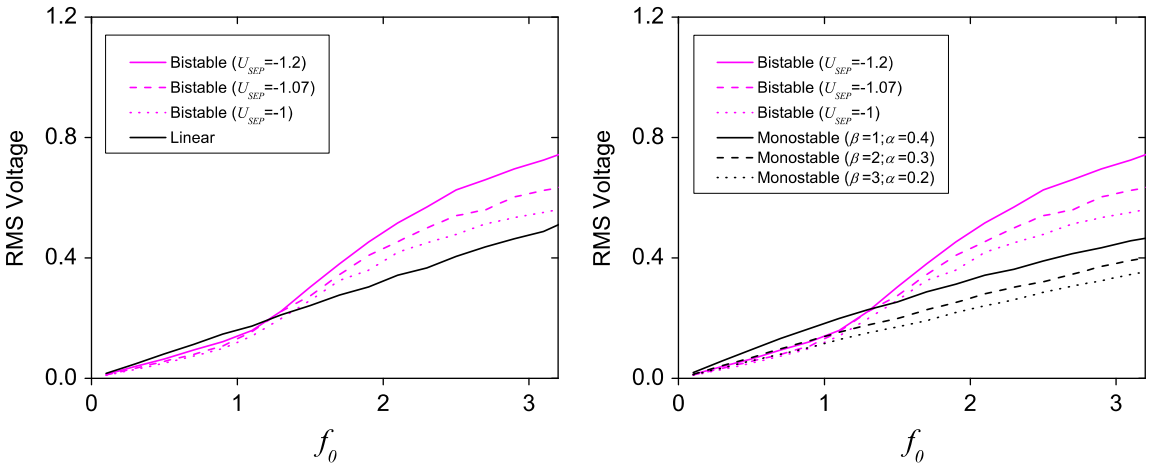

Fig. 4. RMS voltage obtained from linear and nonlinear systems.

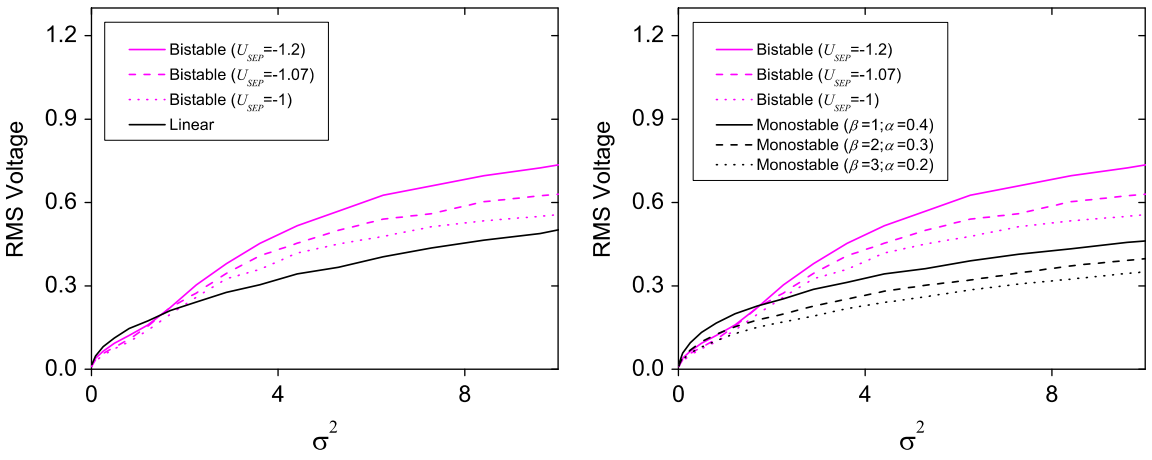

Fig. 5. RMS voltage obtained from linear and nonlinear systems.

once the variance of $n(t)$ is constant, with value 1. Thus, the increase of the variance is associated with an increase of f_0, nevertheless, this is not a general case. By comparing linear and bistable systems (left), we observe a better performance of the bistable system for higher forcing magnitude. The same behavior happens when comparing the bistable system with the monostable (right).

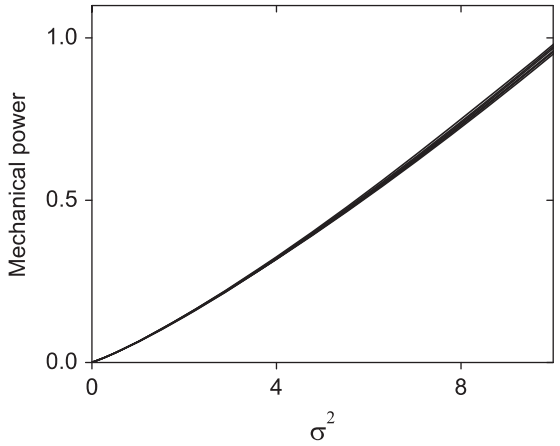

Fig. 6. Effective mechanical power value.

Fig. 6 presents the mechanical power effective value with respect to the variance of the excitation, σ^2, in all analyzed systems. Note that only one curve is observed, once the mechanical power values, provided in all situations, are similar. Since the increase of variance is associated with an increase of forcing magnitude, the analysis is always presented in terms of variance. This choice is based on the fact that this quantity is easier to determine experimentally. Fig. 7 presents the obtained electrical power effective value obtained from linear, nonlinear bistable and nonlinear monostable systems, while Fig. 8 shows the efficiency in power conversion. As expected, an increase in the provided mechanical power leads to an increase in the obtained electrical power, as observed in Figs. 6 and 7. From Fig. 8 a noticeable increase in the efficiency of power conversion by bistable system for greater forcing amplitudes is observed. Note that the efficiency is presented in [%]. For $\sigma^2 = 10$, the bistable system efficiency with $U_{SEP} = -1.2$ presents an increase of 252% when compared to linear case and of 282% when compared to monostable system with $\beta = 1$ and $\alpha = 0.4$.

Fig. 9 shows the time history of the tip displacement of the beam and the voltage provided by the piezoelectric element when a linear system is considered ($\beta = 1.5$ and $\alpha = 0$) for $\sigma^2 = 0.64$ ($f_0 = 0.8$), while Fig. 10 shows the same result for a nonlinear bistable system with $U_{SEP} = -1$ ($\beta = -2.0$ and $\alpha = 1.0$). The nonlinear system has two stable equilibrium points (at $x = -1$ and $x = 1$), and from Fig. 10 (left) we observe that the motion is around only one of them.

Now a greater value of forcing magnitude is considered, $f_0 = 2.4$, resulting in a variance of $\sigma^2 = 5.76$. Fig. 11 shows tip displacement and the provided voltage by the linear system ($\beta = 1.5$ and $\alpha = 0$), while Fig. 12 presents the same result for the nonlinear bistable system with $U_{SEP} = -1$ ($\beta = -2.0$ and $\alpha = 1.0$). For this greater excitation amplitude, the nonlinear system visits both stable equilibrium points as shown in Fig. 12. Note that greater instantaneous values of voltage occur when the tip of the beam jumps from one stable equilibrium point to the other. When the system vibrates around only one equilibrium point, the maximum generated voltage is around 0.4, while when the system jumps from one equilibrium point to the other, the voltage reaches 1.5.

2.2. Experimental analysis

In this section experimental results are presented. The power spectral density (PSD) of acceleration excitation imposed to the beam is shown in Fig. 13. A high-band filter with cut-off frequency of 2.6 Hz is necessary so that the shaker is able to perform the excitation. It is important to highlight that in experimental analysis the dimensional acceleration excitation [m/s] is considered, while in numerical analysis dimensionless forcing magnitude, f_0, and forcing function, $n(t)$, are considered.

Fig. 14 presents the provided RMS voltage of linear, nonlinear bistable and nonlinear monostable systems for different variance of the excitation. Experimental results present the same trend of those obtained from numerical simulations, shown in Fig. 5.

Fig. 15 shows beam's tip displacement of linear system (left) and of bistable system with $d = 30$ mm (right) for $\sigma^2 = 0.15$. Fig. 16 presents the same results for $\sigma^2 = 0.38$. Experimental data confirm numerical simulations showing that higher voltage is provided by bistable system when the tip vibrates around both stable equilibrium points. Note that the generated RMS voltage related to the cases presented in Figs. 15 and 16 are presented in Fig. 14.

Although a quantitative comparison is not performed, it is possible to conclude that numerical simulations capture the general behavior observed in experimental data, presenting a close qualitative agreement.

3. Enhancing the harvested energy in a bistable system

Since the bistable piezomagnetoelastic structure presents the most interesting behavior for energy harvesting purposes, a special attention is dedicated to this system in this section, with the goal of defining suitable excitations that lead to

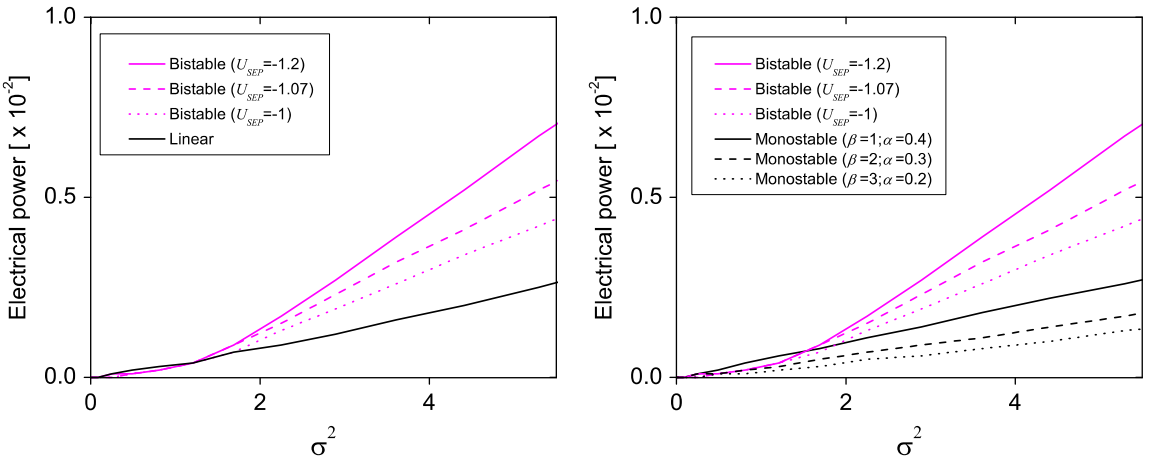

Fig. 7. Electrical power effective value obtained from linear and nonlinear systems.

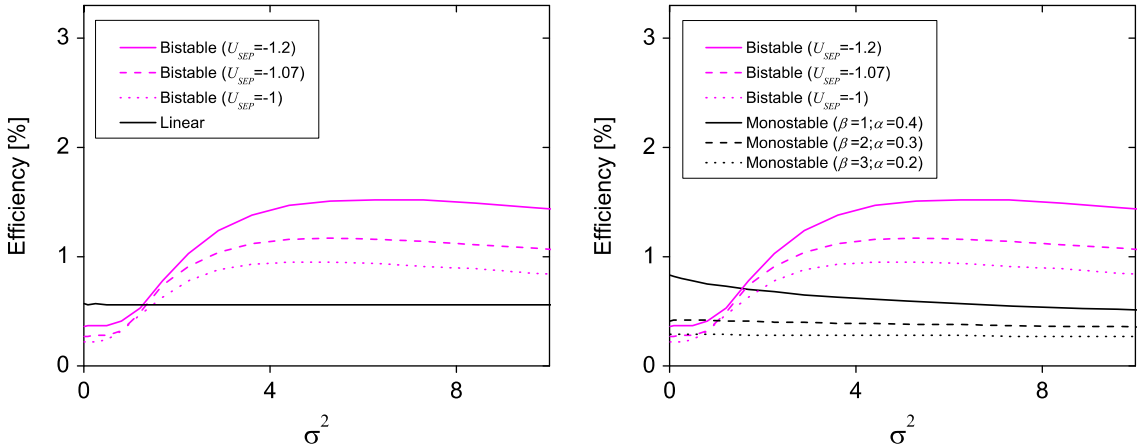

Fig. 8. Power conversion efficiency by linear and nonlinear systems.

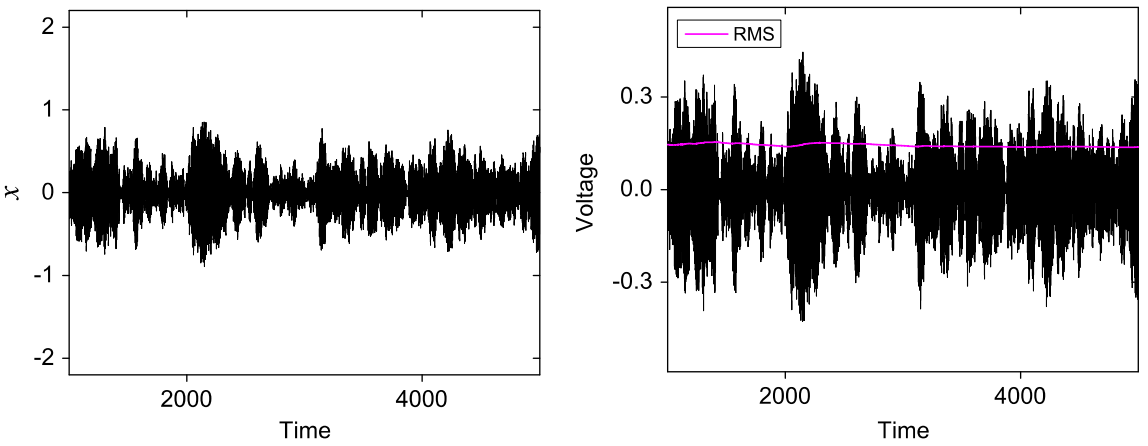

Fig. 9. Linear system response and provided voltage for $\sigma^2 = 0.64$.

enhanced energy harvesting. The structure with $\beta = -2$ and $\alpha = 1$ is investigated. Under this assumption, there are two stable equilibrium points, $x_{SEP} = \pm\sqrt{2}$, and the potential function evaluated at them is $U_{SEP} = -1$. A range of forcing parameter is analyzed and for each forcing magnitude, f_0, simulations are carried out 50 times and $n(t)$ is different in each case. The system is considered to be at rest in one of the stable equilibrium points, half of the time in each SEP. System behavior is analyzed and the percentage of times that the tip oscillates around both SEP in all 50 simulations is represented

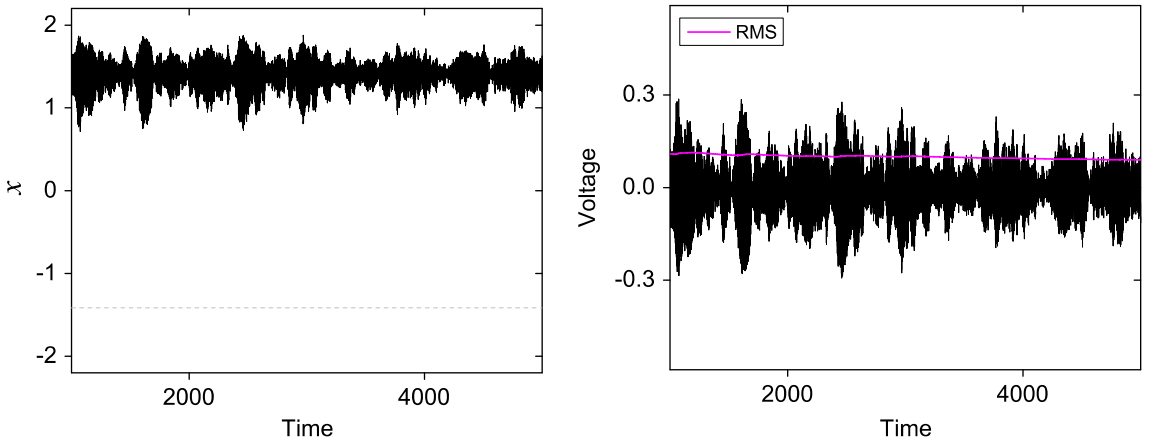

Fig. 10. Nonlinear bistable system ($U_{SEP} = -1$) response and provided voltage for $\sigma^2 = 0.64$.

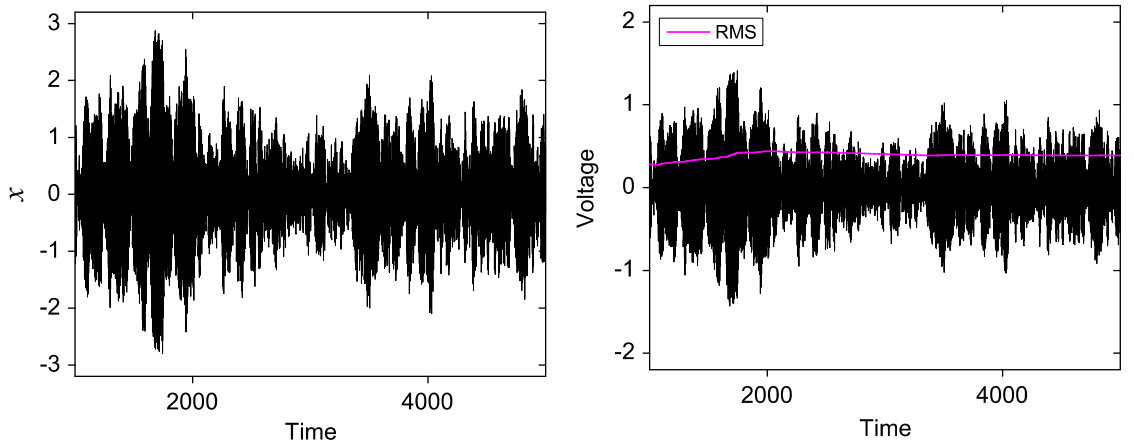

Fig. 11. Linear system response and provided voltage for $\sigma^2 = 5.76$.

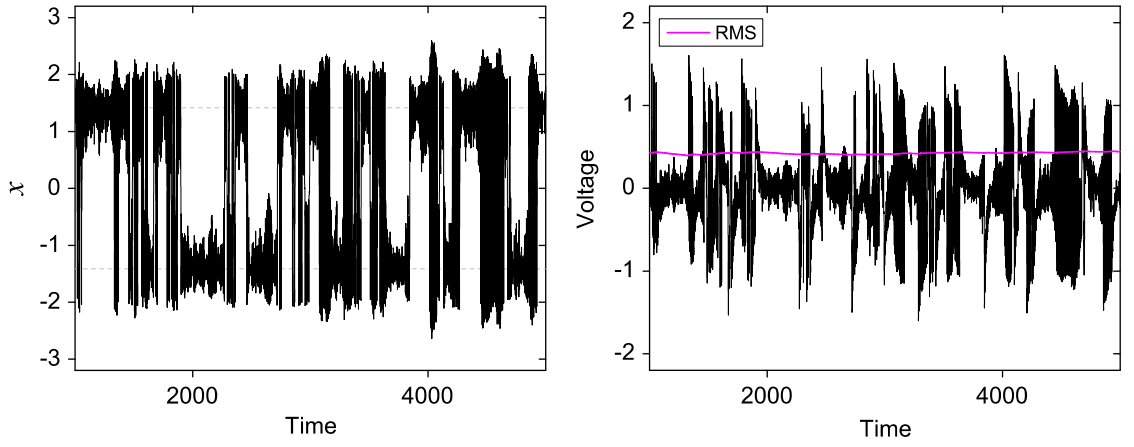

Fig. 12. Nonlinear bistable system ($U_{SEP} = -1$) response and provided voltage for $\sigma^2 = 5.76$.

by a variable, PV_{SEP}, as presented in Fig. 17. This variable is important to characterize when the system presents the desired behavior that enhances the harvested energy. Due to the random excitation, the same value of f_0 can lead to different results. Hence, for the same excitation magnitude the can oscillates around either only one SEP or around both SEP. Three regions are defined: one region where system vibrates around only one SEP ($PV_{SEP} \leq 5\%$), called "One SEP visited"; one region where system vibrates around the two SEP ($PV_{SEP} \geq 95\%$), called "Both SEP visited"; and a transition region, where both situations can occur.

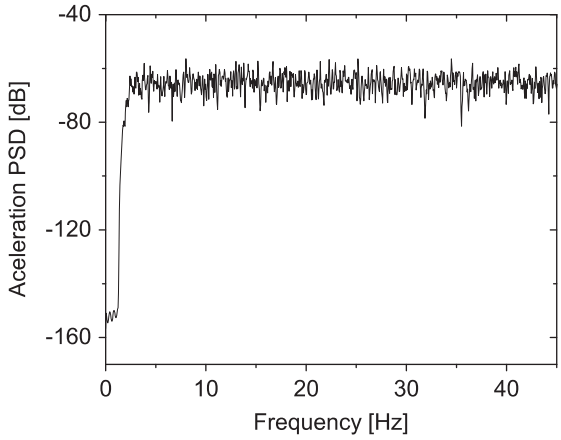

Fig. 13. PSD of experimental excitation acceleration.

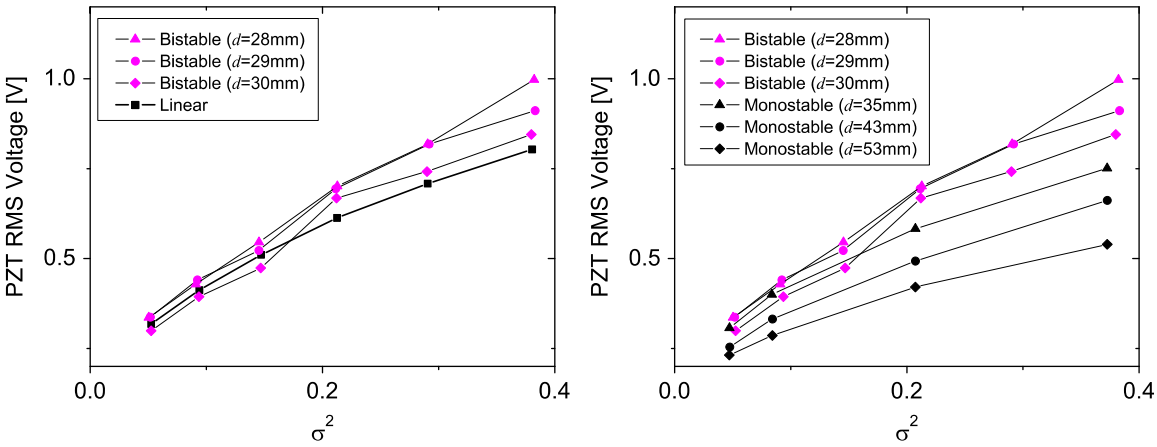

Fig. 14. RMS voltage obtained experimentally from linear and nonlinear systems.

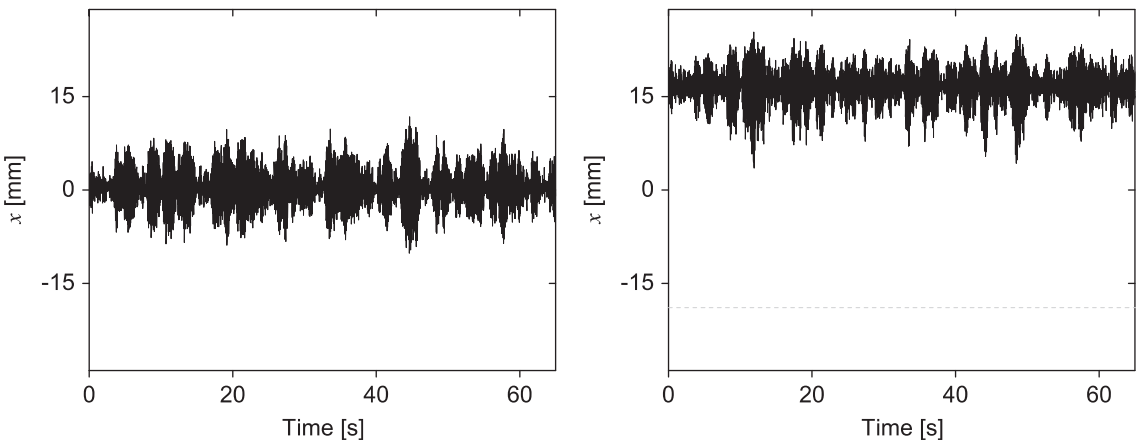

Fig. 15. Tip displacement for $\sigma^2 = 0.15$. Left: linear system; right: bistable system ($d = 30$ mm).

From Figs. 17 and 5, we observe that RMS voltage of nonlinear system becomes greater than the linear system after the transition region. Thus, as verified by Ferrari et al. [10,11] bistable system can improve the provided power, however, this happens only if the tip of the beam oscillates around both stable equilibrium points.

It should be highlighted that the transition region is centralized at $\sigma^2 = 1$. Different values of β and α (related to bistable system) are analyzed presenting a similar pattern. Therefore, the relation between excitation variance and stable equilibrium point potential plays an important role in system dynamics. In Fig. 17, two forcing magnitudes are

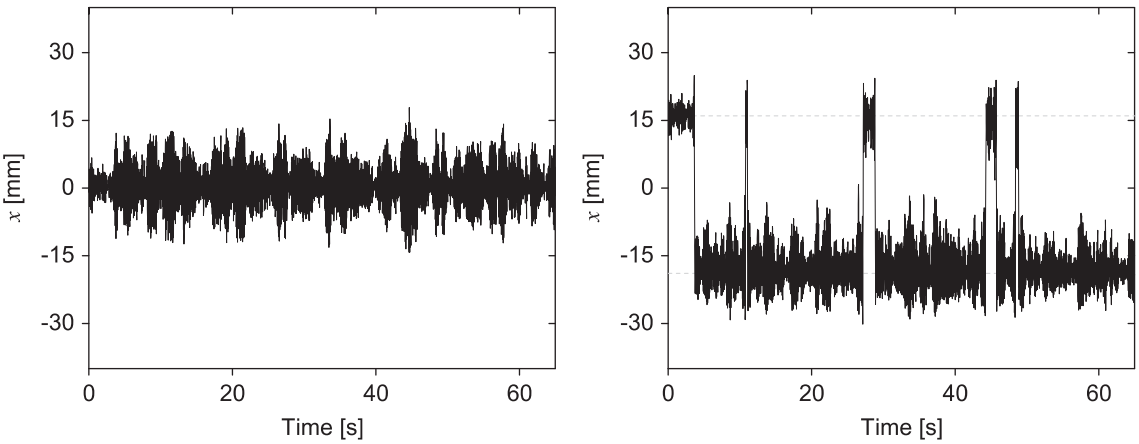

Fig. 16. Tip displacement for $\sigma^2 = 0.38$. Left: linear system; right: bistable system ($d = 30$ mm).

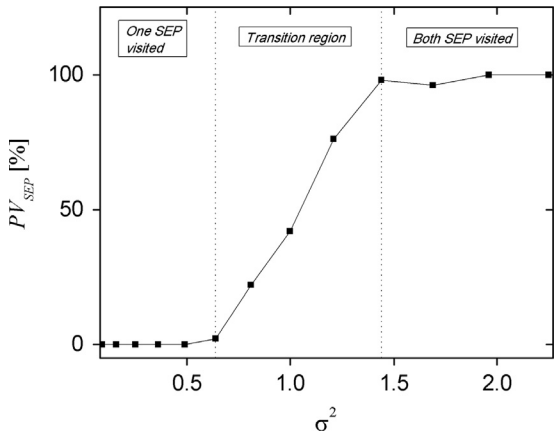

Fig. 17. Percentage of times that system vibrates around both SEP for different variances of excitation.

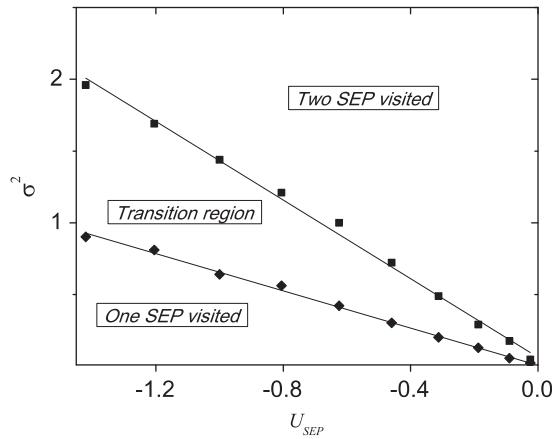

Fig. 18. Relation between excitation variance and U_{SEP} defining three regions.

highlighted: one related to the transition from "One SEP visited" to the transition region ($f_0 = 0.8$ or $\sigma^2 = 0.64$) and the second when occurs at the transition from transition region to the desired behavior where system oscillates around both SEP ($f_0 = 0.8$ or $\sigma^2 = 1.44$).

Fig. 18 presents these two situations for different stable equilibrium potential points (obtained by considering different values of β and α), where '◆' corresponds to the first transition while '■' corresponds to the second transition. Data obtained for each transition is fit by a linear polynomial. Fig. 19 presents similar analysis by considering the absolute value of stable equilibrium point position, x_{SEP}, instead of its potential. In this case, data obtained for each transition is fit to a third order

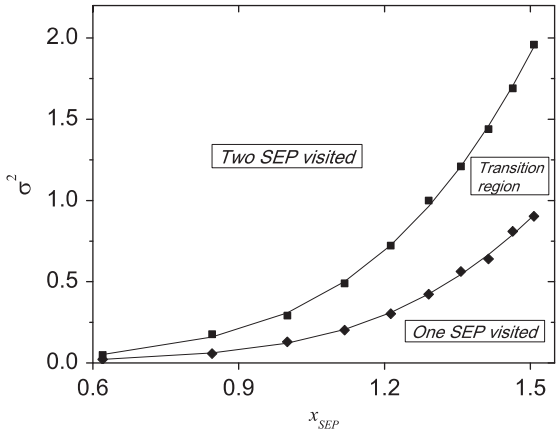

Fig. 19. Relation between excitation variance and x_{SEP} defining three regions.

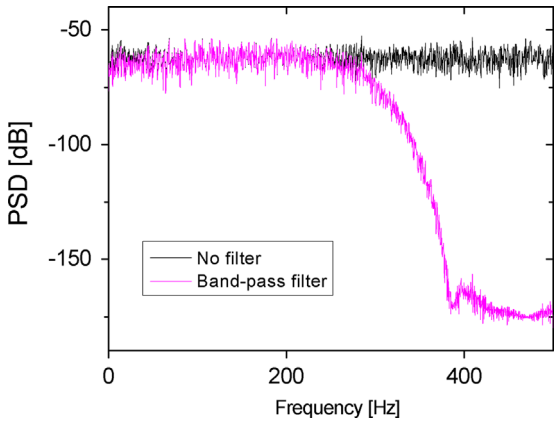

Fig. 20. PSD of the forcing function $n(t)$ without filter and with band-pass filter.

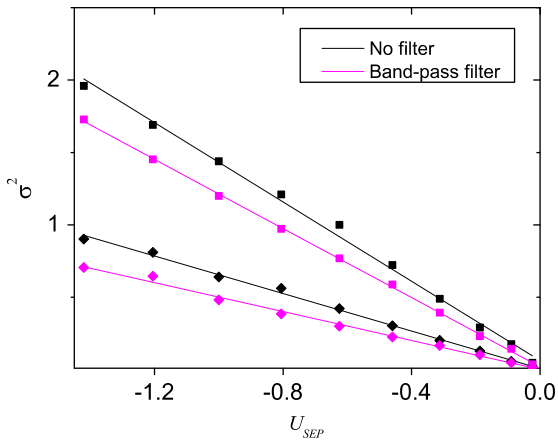

Fig. 21. Relation between excitation variance and U_{SEP} defining the three regions.

polynomial. Results of Fig. 19 are more appropriate for experimental analysis, since it is easier to determine stable equilibrium points position than their potentials. As mentioned before, in the situation presented in Fig. 17, with $\beta=-2$ and $\alpha=1$ (leading to $U_{SEP}=-1$ and $x_{SEP}=1.4142$), the first transition occurs when $\sigma^2=0.64$ and the second when $\sigma^2=1.44$.

Next consider the influence of filtering process. The same analysis presented in Figs. 18 and 19 is investigated by considering the filtered forcing function presented in Fig. 20. Results are presented in Figs. 21 and 22. Note that the transition curves are shifted for smaller values, preserving the general behavior.

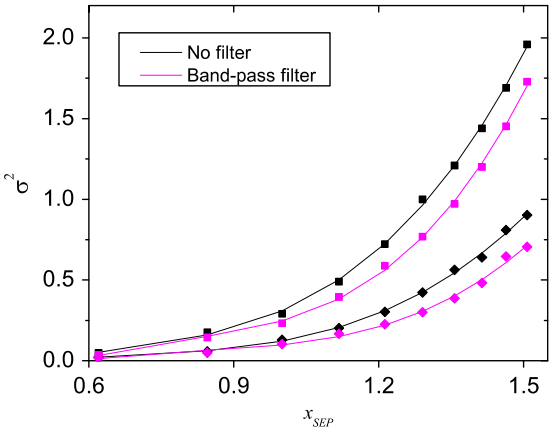

Fig. 22. Relation between excitation variance and x_{SEP} defining the three regions.

4. Conclusions

This work deals with the analysis of the voltage provided by a nonlinear piezomagnetoelastic generator subjected to random excitations. A qualitative analysis was performed using both numerical and experimental information, in order to show that both approaches present the same trend, and define a condition that allows enhanced harvested energy based on quantities that can be easily experimentally identified, e.g., variance of excitation and the coordinates of equilibrium points. Linear, nonlinear bistable and nonlinear monostable systems are compared for different forcing magnitudes, showing a better performance of the bistable system when the tip displacement of the beam oscillates around both stable equilibrium points. Numerical and experimental approaches are carried out showing a good qualitative agreement. Bistable systems present an important relationship between the variance of the excitation and the potential energy that defines energy harvesting enhancement. These relations are quantified for a variety of different potential wells, related to distinct systems, showing a trend between the excitation and potential energy. Three regions are defined: one region where the tip of the beam oscillates around only one stable equilibrium point; the desired region where system jumps from one stable equilibrium point to the other; and a transition regions between these two behaviors. The transition between these three regions is clearly defined for unfiltered and filtered Gaussian noise input, defining the desired region of oscillation. The presented analysis can be useful in the design of energy harvesting system under random excitation. Thus, for a given bistable piezoelectric generator, it is possible define the minimum excitation variance that enhances the harvested energy. Similarly, if a given excitation is provided, it is possible to define bistable system characteristics that enhance the harvested energy.

Acknowledgments

The authors would like to thank the Brazilian Research Agencies CNPq, CAPES and FAPERJ and through the INCT-EIE (National Institute of Science and Technology – Smart Structures in Engineering) the CNPq and FAPEMIG for their support. The authors would like also to acknowledge the support of ANP, FINEP and MCT through PRH-PB/MCT, and also the support of Petrobrás.

References

[1] M.S.M. Soliman, E.M. Abdel-Rahman, E.F. El-Saadany, R.R. Mansour, A wideband vibration-based energy harvester, J. Micromech. Microeng. 18 (2009) 115021.
[2] B. Marinkovic, H. Koser, Smart sand—a wide bandwidth vibration energy harvesting platform, Appl. Phys. Lett. 94 (2009) 103505.
[3] L.V. Blarigan, P. Danzl, J. Moehlis, A broadband vibrational energy harvester, Appl. Phys. Lett. 100 (2012) 253904.
[4] F. Giusaa, A. Giuffridaa, C. Trigonaa, B. Andòa, A.R. Bulsarab, S. Baglio, Random mechanical switching harvesting on inductor: a novel approach to collect and store energy from weak random vibrations with zero voltage threshold, Sens. Actuators A 198 (2013) 35–45.
[5] L. Gammaitoni, I. Neri, H. Vocca, The benefits of noise and nonlinearity: extracting energy from random vibrations, Chem. Phys. 375 (2010) 435–438.
[6] S.M. Shahruz, Increasing the efficiency of energy scavengers by magnets, J. Comput. Nonlinear Dyn. 3 (2008) 041001. (12 pp.).
[7] F. Cottone, H. Vocca, L. Gammaitoni, Nonlinear energy harvesting, Phys. Rev. Lett. 102 (2009) 080601. (4 pp.).
[8] R. Ramlan, M.J. Brennan, B.R. Mace, I. Kovacic, Potential benefits of a non-linear stiffness in an energy harvesting device, Nonlinear Dyn. 59 (4) (2010) 545–558.
[9] A. Erturk, J. Hoffmann, D.J. Inman, A piezomagnetoelastic structure for broadband vibration energy harvesting, Appl. Phys. Lett. 94 (2009) 2541102 (3 pp.).
[10] M. Ferrari, M. Baù, M. Guizzetti, V. Ferrari, A single-magnet nonlinear piezoelectric converter for enhanced energy harvesting from random vibrations, Sens. Actuators A: Phys. 172 (2011) 287–292.
[11] M. Ferrari, V. Ferrari, M. Guizzettia, B. Andòb, S. Bagliob, C. Trigonab, Improved energy harvesting from wideband vibrations by nonlinear piezoelectric converters, Sens. Actuators A: Phys. 162 (2010) 425–431.

[12] A. Erturk, D.J. Inman, A distributed parameter electromechanical model for cantilevered piezoelectric energy harvesters, ASME J. Vib. Acoust. 130 (2008) 041002.
[13] A. Erturk, D.J. Inman, An experimentally validated bimorph cantilever model for piezoelectric energy harvesting from base excitations, Smart Mater. Struct. 18 (2009) 025009.
[14] A. Erturk, O. Bilgen, D.J. Inman, Power generation and shunt damping performance of a single crystal lead magnesium niobate-lead zirconate titanate unimorph: analysis and experiment, Appl. Phys. Lett. 93 (2008) 224102.